VIP Drug Delivery Very Important Paper

DOI: 10.1002/anie.201402144

In Vivo Chemoembolization and Magnetic Resonance Imaging of Liver Tumors by Using Iron Oxide Nanoshell/Doxorubicin/Poly(vinyl alcohol) Hybrid Composites**

Yi-Xiang J. Wang, Xiao-Ming Zhu, Qi Liang, Christopher H. K. Cheng, Wei Wang,* and Ken Cham-Fai Leung**

Abstract: *A hybrid composite made up of superparamagnetic iron oxide nanoshells encapsulating the anticancer drug doxorubicin and bound together by poly(vinyl alcohol) was developed. Transcatheter arterial delivery in an in vivo liver tumor model led to embolization of the liver tumor blood vessels. Embolization was followed by disassembly of the composite. The nanoshells were then able to pass through the leaky tumor vasculature into the tumor tissue, thereby leading to slow and sustained release of the drug. As well as being relatively noncytotoxic, the composite was responsive to magnetic resonance imaging, thus making it a potentially useful theranostic agent.*

Embolization is a procedure commonly used in interventional oncology. Transarterial chemoembolization (TACE) has been shown to provide a survival benefit for liver cancer patients. TACE combines targeted chemotherapy with the effect of ischemic necrosis induced by arterial embolization. Recently, efforts to improve the delivery of chemotherapeutic agents to tumors have led to the development of drug-eluting particles. To avoid the limitation of external beam irradiation that results from the radiosensitive nature of normal hepatic tissue, a minimally invasive transarterial radioembolization technique has been developed and it has proven to be safer in advanced liver cancers. Such agents are currently under clinical evaluation.[1] Key clinical trials for transcatheter arterial therapy for liver cancer[2–5] and the recent patents relevant to cancer chemoembolization are being developed. Herein, we describe the use of a hybrid nanoshell/drug/polymer composite as a chemoembolization agent for transarterial delivery in liver tumors.

To avoid reticuloendothelial system (RES) clearance, the relatively large drug/nanoparticle composites were delivered intra-arterially. Once inside the arterial vessel, the composites will be put under pressure and will effectively block the tumor blood vessels without leaking into the blood stream. We proposed a superparamagnetic iron oxide (SPIO) nanoshell-based[6] chemoembolization hybrid composite[7,8] for transcatheter anticancer drug delivery,[9,10] particularly for liver malignancies (Figure 1). For the chemoembolization composite, hollow superparamagnetic iron oxide nanoshells (139.8 ± 2.7 nm in diameter; Figure S1 in the Supporting Information), the anticancer drug doxorubicin (DOX), and poly(vinyl

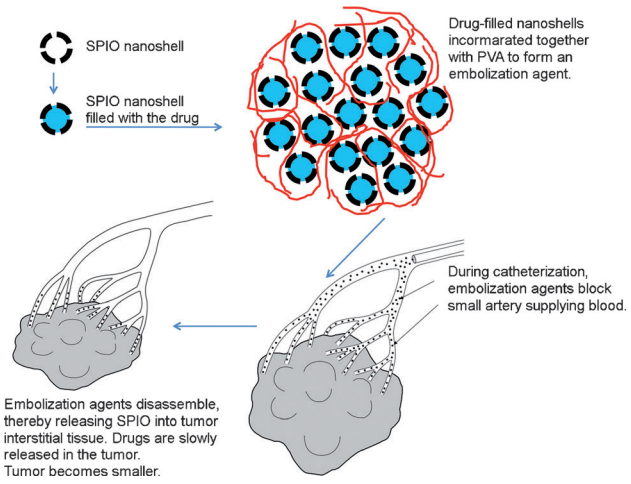

Figure 1. Schematic diagram of hollow superparamagnetic iron oxide (SPIO) nanoshell-based chemoembolization composites for transcatheter anticancer drug delivery. Step 1: synthesis of hollow nanoshells; Step 2: encapsulation of an anticancer drug (blue) into the nanoshells; Step 3: incorporation of drug-filled nanoshells with PVA (red) to give 0.5–1 mm chemoembolization composites; Step 4: chemoembolization composites delivered through a catheter to embolize the arteries supplying blood to the tumor; Step 5: After a period of time, the chemoembolization composite dissembles and the nanoshells pass through the leaky tumor vasculature into the tumor tissue, thereby resulting in the anticancer drugs being released within the tumor.

[*] Dr. X.-M. Zhu, Prof. Dr. K. C.-F. Leung
Department of Chemistry, Institute of Creativity, and State Key Laboratory of Environmental and Biological Analysis
The Hong Kong Baptist University
Kowloon Tong, Kowloon, Hong Kong SAR (P. R. China)
E-mail: cfleung@hkbu.edu.hk

Prof. Dr. Y.-X. J. Wang, Dr. X.-M. Zhu
Department of Imaging and Interventional Radiology, Prince of Wales Hospital, The Chinese University of Hong Kong
Shatin, NT, Hong Kong SAR (P. R. China)
E-mail: yixiang_wang@cuhk.edu.hk

Q. Liang, Prof. Dr. W. Wang
Department of Radiology, Xianya Third Hospital
Central South University, Changsha, Hunan (P. R. China)
E-mail: cjr.wangwei@vip.163.com

Prof. Dr. C. H. K. Cheng
School of Biomedical Sciences
The Chinese University of Hong Kong
Shatin, NT, Hong Kong SAR (P. R. China)

[**] This work was partially supported by Innovation Technology Fund (ITS/066/09) and RGC-General Research Fund (201213). Prof. Guoliang Shao, Department of Radiology, Zhejiang Cancer Hospital is gratefully acknowledged.

Supporting information for this article is available on the WWW under http://dx.doi.org/10.1002/anie.201402144.

alcohol) (PVA) polymers were used. PVA polymers of two degrees of hydrolysis (80 and 98 percent hydrolyzed) were used. The ratio of PVA80 (M_w: 9k–10k Da) to PVA98 (M_w: 31k–50k Da) was optimized to 2:1 w/w for controlling the disintegration rate of the PVA polymers in physiological solutions. PVA80 has higher water solubility than PVA98 (Figure S2). Doxorubicin molecules were encapsulated in the magnetic nanoshells and the PVA polymers glued the drug-encapsulated nanoshells together to form embolization particles of 0.5 to 1.0 mm, which were produced through refining the freeze-dried composite particles of 1.5–2.0 mm (Figure 2 (inset), Figures S3, S4). The DOX loading in the composite

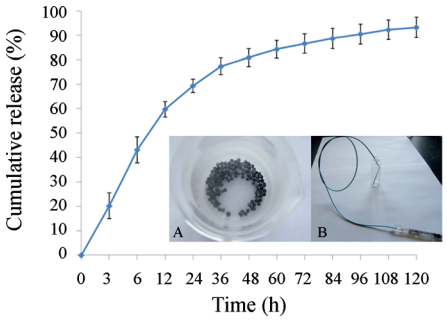

Figure 2. Release profile of doxorubicin from the nanoshell/DOX/PVA composites. The profile shows relatively slow and sustained drug release over 120 h (37 °C, PBS). Inset figures: A) Embolization particles containing nanoshell/DOX/PVA composites, B) Composite embolization particles being passed through a catheter for selective hepatic artery drug delivery.

was determined to be 10 ± 2 weight %. As a proof of concept, these nanoshell/DOX/PVA composite particles were delivered through a catheter selectively placed into a feeding artery of a liver tumor in a rabbit hepatic VX-2 tumor model. The composite particles were released from the catheter, after which they blocked the feeding artery of the tumor. After a period of time (in days), upon the slow disintegration of the PVA polymers, the DOX-encapsulated nanoshells were released and started moving downstream. Thereafter, nanoshells can be transferred through the leaky tumor vasculature into the tumor tissue and the anticancer DOX drugs were released within the tumor. An in vitro drug-release study showed that doxorubicin loaded in the SPIO nanoshells was released gradually from the composite. Owing to the magnetic properties of SPIOs, this composite could induce magnetic resonance imaging (MRI) contrast. Therefore, this composite is a theranostic[11–19] chemoembolization agent.

The release of DOX from the nanoshell/DOX/PVA hybrid composites was monitored by UV/Vis spectroscopy at the local maximum absorption of DOX in the visible region. The release profile shows slow and sustained DOX release from the composite (Figure 2). There is a a plateau at 90 % accumulative release over 120 h at 37 °C in PBS. The slow and sustained drug release provides a one-time dose-controlled therapeutic advantage after surgical chemoembolization. Because of the different solubilities of PVA80 and PVA98, the combination of PVA80 and PVA98 at different ratios gives the possibility to tune the DOX release rate in the composite.

The efficacy of the nanoshell/DOX/PVA hybrid composites for in vivo chemoembolization can be characterized by digital subtraction angiographs. In Figure 3, the blood vessels

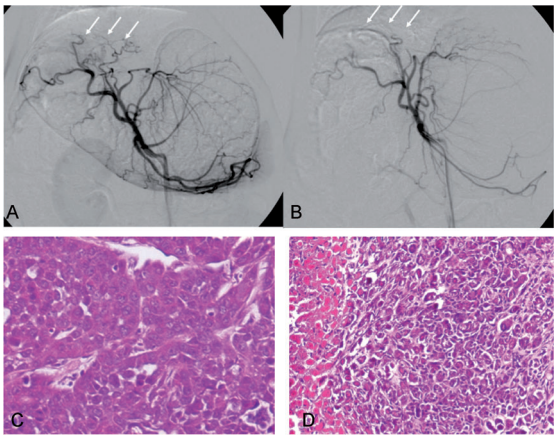

Figure 3. Digital subtraction angiographs before (A) and after (B) in vivo embolization with the nanoshell/DOX/PVA composites in rabbit I. The white arrows indicate the tumor blood vessels. After chemoembolization with the nanoshell/DOX/PVA composites, the tumor blood vessels disappear. Histological evaluation of the VX-2 tumor before (C) and after (D) in vivo embolization with the nanoshell/DOX/PVA composites for 4 days.

supplying a liver VX-2 tumor can be clearly seen. After intra-arterial embolization, those blood vessels had disappeared, thus demonstrating blocking of the blood supply to the tumor. Histology provides further proof of the chemoembolization efficacy based on structural differences in the tumor tissue before (Figure 3 C) and after (Figure 3 D) in vivo chemoembolization of the liver VX-2 tumor for 4 days. In the safety assessment in rats, after chemoembolization, others sites (heart, vertebra, knee, brain, and lung) were analyzed by histology (Figures S7, S8). These tissues did not show changes, thus demonstrating that the composite does not have a toxic effect on these sites after embolization.

The location of the VX-2 liver tumor in a rabbit (rabbit II) can be imaged by using MRI (Figure 4 A, B, C). The SPIO nanoshell-based composites are superparamagnetic and thus produce an enhanced dark contrast in MRI. After chemoembolization by the composite in rabbit II, multiple susceptibility dots with dark contrast can be observed (Figure 4 D, E, F). The livers of two rabbits (I and II) were dissected out after 4 days of chemoembolization with the composites and they showed a paled segment at the location of tumor (Figure 4 G, H) in the liver. This is because the tumors are devoid of blood supply and also show the appearance of necrosis based on the slow/sustained release and action of the anticancer drug DOX.

A hemolysis assay was performed with the nanoshells. As summarized in Table 1, the hemolysis percentages of rabbit erythrocytes incubated for 3 h at 37 °C with the nanoshells at different iron concentrations were determined to be insignificant. Erythrocytes are thus not ruptured by the composite.[20]

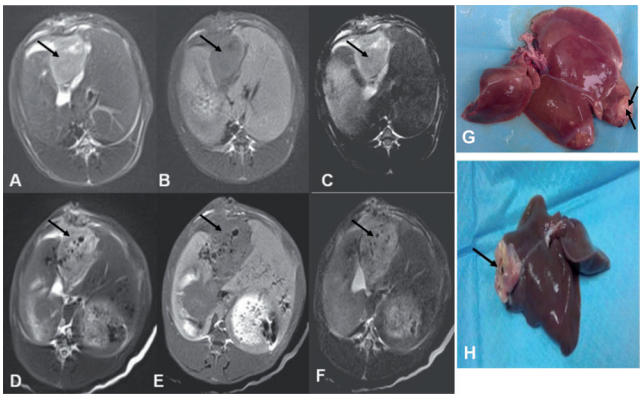

Figure 4. MRI of rabbit II before (A–C) and after (D–F) chemoembolization. The arrows indicate the VX-2 tumor in the liver. After chemoembolization with the nanoshell/DOX/PVA composites, multiple susceptibility (dark contrast) dots are observed in the VX-2 tumor region. Macroscopic views of the VX-2 tumor in the liver after chemoembolization with the nanoshell/doxorubicin/PVA composites are shown for rabbit I (G) and rabbit II (H) after 4 days. The tumors (indicated by arrows) are devoid of blood supply and thus appear pale and show the appearance of necrosis.

Table 1: Hemolysis percentage of rabbit erythrocytes incubated at 37 °C for 3 h with different concentrations of the nanoshells.

Iron concentration of SPIO nanoshells [μg mL^{-1}]	Hemolysis [%]
0	0
6.25	0.04 ± 0.49
12.5	0.33 ± 0.58
25	−0.35 ± 0.49
50	−0.21 ± 0.45
100	0.16 ± 0.70

Cell viability following exposure to the composite for 24 h at different iron concentrations was evaluated for macrophage RAW264.7 (Figure 5A) and fibroblast L929 cells (Figure 5B). The nanoshells are relatively nontoxic toward these cells at the working concentration range and even at 100 μg(Fe)/mL. The cell adhesion evaluations of the nanoshell-exposed fibroblast L929 (Figure 5C) and Chinese hamster ovary CHO-K1 (Figure S9) cells show insignificant cytotoxicity. Cell-proliferation evaluation with fibroblast L929 cells in the presence of the nanoshells demonstrates approximately 90% cell viability after 3 days of incubation (Figure 5D). However, cell-proliferation evaluation with Chinese hamster ovary cells CHO-K1 incubated with the nanoshells showed a slight reduction in cell viability to approximately 80% after 3 days (Figure S10).[21,22]

In summary, the embolization of rabbit liver VX-2 tumors with superparamagnetic iron oxide nanoshell/doxorubicin/poly(vinyl alcohol) composite particles confirmed the feasibility of transcatheter delivery of the composite particles, their embolization effect (leading to tumor necrosis), and the feasibility of MRI monitoring of the distribution of the composite particles after delivery. The slow and sustained drug release provides a one-time dose-controlled therapeutic advantage after surgical chemoembolization. Because of the

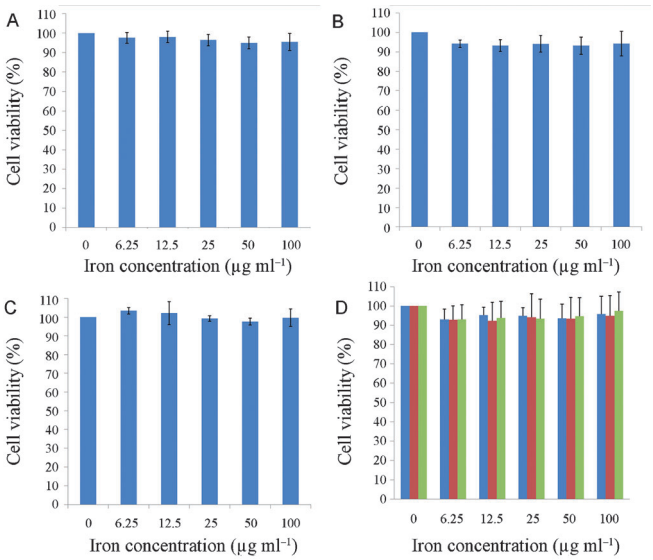

Figure 5. Cell viability of macrophage RAW264.7 (A) and fibroblast L929 (B) cells incubated with the nanoshells for 24 h. C) Cell adhesion of fibroblast L929 cells incubated with the nanoshells for 4 h. D) Cell proliferation of fibroblast L929 cells incubated with the nanoshells at different iron concentrations after 1 (blue), 2 (red), and 3 (green) days of exposure.

different solubilities of PVA80 and PVA98, the combination of PVA80 and PVA98 at different ratios gives the possibility to tune the rate of DOX release from the composite. The as-prepared composite was relatively noncytotoxic and MRI-responsive, thus rendering it a novel theranostic chemoembolization agent. Since the composite disintegrates into noncytotoxic components (PVA and empty SPIO nanoshells), it is envisaged that these would eventually be excreted from the body.[23] The excretion kinetics could be further confirmed by monitoring the concentration and location of the SPIO nanoshells by MRI.

Experimental Section

Ferric chloride, poly(vinyl alcohol) (PVA80: 80% hydrolysed, M_w 9k–10k Da; PVA98: 98% hydrolysed, M_w: 31k–50k Da), and other reagents were purchased from Sigma–Aldrich. Doxorubicin hydrochloride was purchased from Zhejiang Hisun Pharmaceutical Co. Ltd. Iron concentrations were determined by inductively coupled plasma optical emission spectroscopy (ICP-OES, Optima 4300 DV). Transmission electron microscopy (TEM) images were taken on a FEI CM120 microscope at an accelerating voltage of 120 kV and a high-resolution transmission electron microscope (HRTEM, Tecnai F20, FEI) at an accelerating voltage of 200 kV.

A one-pot hydrothermal method was used to prepare the hollow superparamagnetic iron oxide nanoshells according to reported procedures.[6] Polymer hybrids were prepared by gently heating PVA80/PVA98 (2:1 w/w) in water. The completely dissolved polymer solution was mixed with doxorubicin-loaded nanoshells and the resulting solution was introduced in single droplets into liquid nitrogen by using a syringe with 27 G size needle. The frozen droplets were immediately transferred into a flask and freeze-drying was performed for 2 days to remove the water from the particles.

Cells were obtained from American Type Culture Collection (ATCC, Manassas, VA). Cells were cultured in Dulbecco's modified

Eagle's medium (DMEM; Life Technologies) containing 10% fetal bovine serum (FBS), 100 U mL^{-1} penicillin, and 100 μg mL^{-1} streptomycin at 37 °C and in a humidified 5% CO_2 atmosphere.

Biocompatibility assay: The cytotoxicity of the different nanoshells was examined by methylthiazolyldiphenyltetrazolium bromide (MTT) assay in the cells. A total of 5000 or 10000 cells were seeded onto the wells of a 96-well plate. After incubation for 12 h, the medium in the wells was replaced with 100 μL DMEM containing different concentrations of nanoshells. Then, 10 μL of 5 mg mL^{-1} MTT was added into each well. After incubation for 3 h, the medium was removed and formazan crystals were dissolved in dimethyl sulfoxide (150 μL) for 10 min on a shaker. A circular disc-like magnet was placed under the plate to attract the cells, which had taken up the magnetic nanoshells, to the bottom of the well. 100 μL of the supernatant was transferred to another 96-well plate. The absorbance of each well was measured on a microplate reader (Bio-Rad, Model 3550) at a wavelength of 540 nm. The relative cell viability (%) for each sample related to control well was calculated.

In vitro hemolysis assay: Rabbit erythrocytes were collected by centrifugation at 1500 rpm for 10 min and then washed three times with PBS buffer at pH 7.4. The stock dispersion was prepared by mixing 3 mL of centrifuged erythrocytes into 11 mL of PBS. The nanoshell dispersions were prepared in PBS buffer at concentrations 6.25–100 μg mL^{-1}. 100 μL of stock dispersion was added to 1 mL of the nanoshell dispersions. The solutions were mixed and incubated for 3 h at 37 °C. 200 μL of solution was transferred to a 96-well plate for measurement of absorbance at 540 nm. Percentage hemolysis was calculated according to $(A_S - A_N)/(A_P - A_N)\,100\,\%$, where A_S is the absorbance resulting from addition of the SPIO nanoshells to the erythrocyte suspension, A_N is the absorbance following the addition of PBS buffer as a negative control, and A_P is the absorbance following the addition of distilled water as a positive control.

New Zealand White rabbits with the VX-2 tumor model implanted in the liver were used for the in vivo study. MRI of the liver was carried out after the rabbits were anesthetized. The right femoral artery of the rabbit was cannulized with a catheter, and under the guidance of DSA (digital subtraction angiography), the catheter was selectively advanced to the hepatic artery branch that supplies the VX-2 tumor. To embolize the hepatic artery branch, SPIO/doxorubicin/PVA composite particles were released from the catheter; the doxorubicin dosage was set to be 1 mg kg^{-1} weight. After the SPIO/doxorubicin/PVA composite particles were delivered, radiographic contrast agent was injected into the catheter to confirm the completeness of embolization. After the embolization procedure, the right femoral artery was repaired and MR imaging of the liver was performed again to determine the distribution of SPIO/doxorubicin/PVA composite particles.

MRI was performed with a Philips Medical Systems 3.0-T clinical whole-body magnetic resonance unit. An 8-channel knee radio-frequency coil was used as the signal transmitter and receiver. Axial spin echo T1-weighted and T2-weighted images of the liver were obtained. The thickness was 2 mm with an interval slice gap of 0.3 mm. Respirator gating was used with time of repetition between 2010 and 4200 milliseconds and time of echo in 43 milliseconds. The Field of view (FOV) was 150 mm and the scan matrices were 256 × 256. The number of excitations was four.

Received: February 7, 2014
Published online: March 25, 2014

Please note: Minor changes have been made to this manuscript since its publication in *Angewandte Chemie* Early View. The Editor.

Keywords: antitumor agents · chemoembolization · drug delivery · iron oxide · liver cancer

[1] K. Y. Tam, K. C.-F. Leung, Y.-X. J. Wang, *Eur. J. Pharm. Sci.* **2011**, *44*, 1 – 10.
[2] J. Lu, S. Ma, J. Sun, C. Xia, C. Liu, Z. Wang, X. Zhao, F. Gao, Q. Gong, B. Song, X. Shuai, H. Ai, Z. Gu, *Biomaterials* **2009**, *30*, 2919 – 2928.
[3] K. C.-F. Leung, C.-P. Chak, S.-F. Lee, J. M. Y. Lai, X.-M. Zhu, Y.-X. J. Wang, K. W. Y. Sham, C.-H. Wong, C. H. K. Cheng, *Chem. Asian J.* **2013**, *8*, 1760 – 1764.
[4] K. C.-F. Leung, S.-F. Lee, C.-H. Wong, C.-P. Chak, J. M. Y. Lai, X.-M. Zhu, Y.-X. J. Wang, K. W. Y. Sham, C. H. K. Cheng, *Methods* **2013**, *64*, 315 – 321.
[5] K. C.-F. Leung, C.-H. Wong, X.-M. Zhu, S.-F. Lee, K. W. Y. Sham, J. M. Y. Lai, C.-P. Chak, Y.-X. J. Wang, C. H. K. Cheng, *Quant. Imaging Med. Surg.* **2013**, *3*, 302 – 307.
[6] X.-M. Zhu, J. Yuan, K. C.-F. Leung, S.-F. Lee, K. W. Y. Sham, C. H. K. Cheng, D. W. T. Au, G.-J. Teng, A. T. Ahuja, Y.-X. J. Wang, *Nanoscale* **2012**, *4*, 5744 – 5754.
[7] K. C.-F. Leung, C.-P. Chak, S.-F. Lee, J. M. Y. Lai, X.-M. Zhu, Y.-X. J. Wang, K. W. Y. Sham, C. H. K. Cheng, *Chem. Commun.* **2013**, *49*, 549 – 551.
[8] Y. Lee, K. Miyata, M. Oba, T. Ishii, S. Fukushima, M. Han, H. Koyama, N. Nishiyama, K. Kataoka, *Angew. Chem. Int. Ed.* **2008**, *47*, 5163 – 5166; *Angew. Chem.* **2008**, *120*, 5241 – 5244.
[9] J.-H. Lee, K.-J. Chen, S.-H. Noh, M. A. Garcia, H. Wang, W.-Y. Lin, H. Jeong, B. J. Kong, D. B. Stout, J. Cheon, H.-R. Tseng, *Angew. Chem. Int. Ed.* **2013**, *52*, 4384 – 4388; *Angew. Chem.* **2013**, *125*, 4480 – 4484.
[10] S.-F. Lee, X.-M. Zhu, Y.-X. J. Wang, S.-H. Xuan, Q. H. You, W.-H. Chan, C.-H. Wong, F. Wang, J. C. Yu, C. H. K. Cheng, K. C.-F. Leung, *ACS Appl. Mater. Interfaces* **2013**, *5*, 1566 – 1574.
[11] D. F. Moyano, V. M. Rotello, *Langmuir* **2011**, *27*, 10376 – 10385.
[12] M. W. Ambrogio, C. R. Thomas, Y.-L. Zhao, J. I. Zink, J. F. Stoddart, *Acc. Chem. Res.* **2011**, *44*, 903 – 913.
[13] H. Yan, C. Teh, S. Sreejith, L. Zhu, A. Kwok, W. Fang, X. Ma, K. T. Nguyen, V. Korzh, Y. L. Zhao, *Angew. Chem. Int. Ed.* **2012**, *51*, 8373 – 8377; *Angew. Chem.* **2012**, *124*, 8498 – 8502.
[14] S. S. Kelkar, T. M. Reineke, *Bioconjugate Chem.* **2011**, *22*, 1879 – 1903.
[15] W. R. Algar, D. E. Prasuhn, M. H. Stewart, T. L. Jennings, J. B. Blanco-Canosa, P. E. Dawson, I. L. Medintz, *Bioconjugate Chem.* **2011**, *22*, 825 – 858.
[16] B. A. Smith, B. D. Smith, *Bioconjugate Chem.* **2012**, *23*, 1989 – 2006.
[17] K. C.-F. Leung, S. Xuan, X. Zhu, D. Wang, C.-P. Chak, S.-F. Lee, W. K.-W. Ho, B. C.-T. Chung, *Chem. Soc. Rev.* **2012**, *41*, 1911 – 1928.
[18] H. Ke, J. Wang, Z. Dai, Y. Jin, E. Qu, Z. Xing, C. Guo, X. Yue, J. Liu, *Angew. Chem. Int. Ed.* **2011**, *50*, 3017 – 3021; *Angew. Chem.* **2011**, *123*, 3073 – 3077.
[19] K. Hayashi, M. Nakamura, W. Sakamoto, T. Yogo, H. Miki, S. Ozaki, M. Abe, T. Matsumoto, K. Ishimura, *Theranostic* **2013**, *3*, 366 – 376.
[20] I. P. Lau, H. Chen, J. F. Wang, H. C. Ong, K. C.-F. Leung, H. P. Ho, S. K. Kong, *Nanotoxicology* **2012**, *6*, 847 – 856.
[21] X.-M. Zhu, Y.-X. J. Wang, K. C.-F. Leung, S.-F. Lee, F. Zhao, D.-W. Wang, J. M. Y. Lai, C. Wan, C. H. K. Cheng, A. T. Ahuja, *Int. J. Nanomed.* **2012**, *7*, 953 – 964.
[22] Q. Mu, N. S. Hondow, L. Krzeminski, A. P. Brown, L. J. C. Jeuken, *Part. Fibre Toxicol.* **2012**, *9*, 29.
[23] X. He, H. Nie, K. Wang, W. Tan, X. Wu, P. Zhang, *Anal. Chem.* **2008**, *80*, 9597 – 9603.

